Biomechanical Changes in the Sclera of Monkey Eyes Exposed to Chronic IOP Elevations

Michaël J. A. Girard,[1,2,3] *J.-K. Francis Suh,*[2,4] *Michael Bottlang,*[5] *Claude F. Burgoyne,*[2,6] *and J. Crawford Downs*[1,2]

Purpose. To characterize scleral biomechanics in both eyes of eight monkeys in which chronic intraocular pressure (IOP) elevation was induced in one eye.

Methods. Each posterior sclera was mounted on a pressurization apparatus, IOP was elevated from 5 to 45 mm Hg while the 3D displacements of the scleral surface were measured by speckle interferometry. Finite element (FE) models of each scleral shell were constructed that incorporated stretch-induced stiffening and multidirectionality of the collagen fibers. FE model predictions were then iteratively matched to experimental displacements to extract unique sets of scleral biomechanical properties.

Results. For all eyes, the posterior sclera exhibited inhomogeneous, anisotropic, nonlinear biomechanical behavior. Biomechanical changes caused by chronic IOP elevation were complex and specific to each subject. Specifically: (1) Glaucomatous eyes in which the contralateral normal eyes displayed large modulus or thickness were less prone to biomechanical changes; (2) glaucomatous scleral modulus associated with an IOP of 10 mm Hg decreased (when compared with that of the contralateral normal) after minimal chronic IOP elevation; (3) glaucomatous scleral modulus associated with IOPs of 30 and 45 mm Hg increased (when compared with that of the contralateral normal) after moderate IOP elevation; and (4) FE-based estimates of collagen fiber orientation demonstrated no change in the glaucomatous eyes.

Conclusions. Significant stiffening of the sclera follows exposure to moderate IOP elevations in most eyes. Scleral hypercompliance may precede stiffening or be a unique response to minimal chronic IOP elevation in some eyes. These biomechanical changes are likely to be the result of scleral extracellular matrix remodeling. (*Invest Ophthalmol Vis Sci.* 2011;52:5656–5669) DOI:10.1167/iovs.10-6927

From the [1]Ocular Biomechanics Laboratory and the [6]Optic Nerve Head Research Laboratory, Devers Eye Institute, Portland, Oregon; the [2]Department of Biomedical Engineering, Tulane University, New Orleans, Louisiana; and the [5]Biomechanics Laboratory, Legacy Research and Technology Center, Portland, Oregon.

Present affiliations: the [3]Department of Bioengineering, Imperial College, London, United Kingdom; and [4]The Center for Bionics Research, Korea Institute of Science and Technology, Seoul, Korea.

Presented in part at the annual meeting of the Association for Research in Vision and Ophthalmology, Fort Lauderdale, Florida, May 2009.

Supported by NIH Grant R01EY11610 (CFB) and the Legacy Good Samaritan Foundation, Portland, OR.

Submitted for publication November 21, 2010; revised February 18, 2011; accepted March 31, 2011.

Disclosure: **M.J.A. Girard**, None; **J.-K.F. Suh**, None; **M. Bottlang**, None; **C.F. Burgoyne**, None; **J.C. Downs**, None

Corresponding author: J. Crawford Downs, Ocular Biomechanics Laboratory, Devers Eye Institute, 1225 NE Second Avenue, Portland, OR 97232; cdowns@deverseye.org.

Glaucoma is the second leading cause of blindness worldwide[1,2] and leads to vision loss through irreversible damage to retinal ganglion cell axons as they pass through the scleral canal at the optic nerve head (ONH). Although glaucoma pathogenesis is not well understood and could also involve direct damage to the retinal ganglion cells or lateral geniculate, the biomechanical environment of the ONH has been hypothesized to play an important role in the neuropathy. The sclera is an important factor in ONH biomechanics, and recent work strongly suggests that the biomechanics of the posterior sclera and lamina cribrosa are tightly coupled.[3–6] The sclera is the stiffest tissue of the eye and provides the mechanical boundary conditions for the lamina cribrosa at its insertion into the scleral canal wall. Computational models have shown that scleral stiffness[7] and scleral collagen fiber organization[3,4] dictate the IOP-induced deformation exhibited by the ONH. Of note, the sclera exhibits significant biomechanical changes with age[8] and after exposure to chronic IOP elevation, as shown herein, both of which are major risk factors in glaucoma.

To investigate scleral biomechanics as a factor in glaucomatous damage, it is important to quantify its mechanical response to IOP. The stresses and strains in the sclera are significant at normal IOPs,[8,9] and exposure to elevated IOP could lead to changes in scleral biomechanics that precede the onset of glaucoma or occur very early in disease progression. We therefore focused this work on the scleral changes that are present at the early stages of the disease in nonhuman primates, which could indicate that scleral biomechanics and its IOP-induced changes contribute to both the individual susceptibility to glaucoma and its pathogenesis.

We recently described our ex vivo method to experimentally measure the 3-D deformation pattern and thickness of posterior sclera from both eyes of four young and four old monkeys after IOP elevation from 5 to 45 mm Hg.[8] In that report, we modeled the posterior sclera as a nonlinear, anisotropic, inhomogeneous soft-tissue using a fiber-reinforced constitutive theory that included stretch-induced stiffening and multidirectionality of the collagen fibers.[3] We then derived eye-specific sets of scleral biomechanical properties based on the experimental observations using an inverse finite element (FE) method.[9] Our results showed that posterior and peripapillary sclera in old monkeys is significantly stiffer than that from young monkeys and is therefore subject to higher stress but lower strain at all levels of IOP. Whether age-related changes in scleral biomechanics contribute to the development and progression of glaucoma remains to be determined.

We have demonstrated significant alterations in the architecture of the laminar and peripapillary scleral connective tissues at the earliest stage of experimental glaucoma (EG) in the monkey eye.[10–18] In the lamina cribrosa of EG monkey eyes, permanent deformation and thickening,[16] accompanied by increases in both total connective tissue volume and total number of laminar beams, were observed.[15] In addition, we

observed posterior deformation accompanied by thinning in the peripapillary sclera in the EG eyes.[13,14] These morphologic changes are likely to result from both physical deformation in response to the applied load (IOP) and connective tissue remodeling in response to chronically elevated stress and strain levels.[15,19,20] Glaucomatous remodeling of the connective tissues by optic nerve head (ONH) astrocytes and scleral fibroblasts may in turn contribute to retinal ganglion cell axonal damage through direct and/or indirect cellular mechanisms.[21,22]

We have shown that the biomechanical properties of the peripapillary sclera are altered in early EG using uniaxial testing and linear viscoelastic theory.[11] That study demonstrated a significant increase in the equilibrium modulus of the peripapillary sclera from glaucomatous monkey eyes, but no changes were seen in the time-dependent viscoelastic parameters in those eyes.

In the present study, we used novel three-dimensional (3-D) experimental and computational techniques[3,8,9] to characterize peripapillary and posterior scleral biomechanics in both eyes of eight adult monkeys in which one eye had been exposed to chronic, laser-induced IOP elevations of modest to substantial magnitude and duration.

Material and Methods

Experiments

Experimental Glaucoma. All experiments adhered to the ARVO Statement for the Use of Animals in Ophthalmic and Vision Research. In this study, EG was induced in one eye of eight rhesus monkeys that had no initial ocular abnormality. Our protocol for generating and detecting laser-induced EG has been fully described in previous reports.[12–14,16] Briefly, both eyes of each monkey underwent IOP measurement (Tonopen XL; Reichert, Depew, NY) and confocal scanning laser tomographic (CSLT) imaging (Heidelberg Retinal Tomograph; Heidelberg Engineering, Heidelberg, Germany) at manometrically controlled IOP of 10 mm Hg on three to five occasions while normal. Then, imaging was performed every 1 to 2 weeks after laser photocoagulation of the trabecular meshwork (OcuLight TX; Iridex, Mountain View, CA) in one eye, until the onset and/or progression of CSLT-detected ONH surface change by mean position of the disc (MPD) or HRT II topographic change analysis (TCA).[23] Four monkeys were observed until the onset of MPD change (confirmed twice), which is our existing criterion for onset of early experimental glaucomatous damage to the ONH.[24] Four additional monkeys were observed up to MPD onset and at least one episode of further progression (confirmed twice) to achieve a more advanced stage of ONH (and presumably scleral) alteration. All the monkeys were killed after an intramuscular injection of ketamine/xylazine with an intravenous injection of pentobarbital sodium.

Cumulative IOP Insult. The load-bearing connective tissues of the posterior sclera directly experience glaucomatous alterations of intraocular pressure,[11] whereas they are likely to be only minimally affected by glaucomatous alterations to the neural and connective tissues of the ONH. We therefore chose to stage the animals by EG eye cumulative IOP insult rather than by the magnitude of MPD or TCA ONH surface change. We defined cumulative IOP insult for each EG eye to be the difference between the area (computed using the trapezoidal rule) under its IOP-time curve (Fig. 1, red) minus that of its contralateral normal eye (Fig. 1, blue;). Monkey 1 therefore received the lowest cumulative IOP insult and monkey 8, the highest (Table 1).

Scleral Mechanical Testing. For this study, we used an experimental protocol for pressure testing the posterior scleral shell that has been fully described in our other reports.[8,9] Briefly, all monkeys were anesthetized with an intramuscular injection of ketamine/xylazine and killed with an intravenous injection of sodium pentobarbital. The eyes were enucleated immediately after death, and the posterior scleral shells were cleaned of intra- and extraorbital tissues and individually mounted on a custom-built pressurization apparatus (see Ref. 9 for a detailed description of the apparatus). After mounting, each shell was blotted dry, covered with a white contrast medium (ProCAD Contrast Medium; Ivoclar, Schaan, Lichtenstein), and immediately immersed in isotonic saline at room temperature. IOP was incrementally increased from 5 to 45 mm Hg, and the resulting full-field 3-D displacements of each shell surface were recorded at a resolution of 0.1 μm with an electronic speckle pattern interferometry sensor[25,26] (Q100; Ettemeyer AG, Ulm, Germany). Internal pressure was then reset to 5 mm Hg, and scleral topography was manually measured with a 3-D digitizing arm (MicroScribe G2X; Immersion, San Jose, CA). Scleral thickness was also measured at 20 predetermined locations (see Ref. 9 for details) with a 20-MHz ultrasound transducer (PacScan 300P; Sonomed, Inc., Lake Success, NY). The topography and thickness data were combined to create an eye-specific reference geometry for the posterior scleral shell in each subject.

Estimation of Scleral Mechanical Properties by Inverse FE Modeling

Our constitutive theory for simulating the biomechanical behavior of the posterior sclera and our inverse FE method of extracting mechanical properties based on the scleral pressure testing outlined above have been fully described in our previous reports.[3,8,9] Both are briefly explained as follows.

Constitutive Theory. We modeled the posterior sclera as a nonlinear, anisotropic, inhomogeneous soft tissue by using fiber-reinforced composite theory. Within this framework, we assume that scleral collagen fibers provide most of the resistance to IOP and are responsible for two important biomechanical characteristics (nonlinearity, described with the parameters c_3 and c_4, and anisotropy, with θ_p and k; Fig. 2). The model assumes that scleral collagen fibers are embedded within a ground substance matrix, not to be confused with the extracellular matrix, which includes all the remaining tissue constituents (e.g., water, fibroblasts, proteoglycans, and elastin). Hence, the ground substance matrix is of low stiffness compared with the collagen fibers, and its mechanical behavior is characterized with a single intrinsic parameter, c_1, as isotropy is assumed (i.e., no preferred orientation).

Inverse FE Modeling. Using our inverse FE method, we estimated a set of thirteen model parameters (c_1, c_3, c_4, k_1, k_2, and θ_{p1} to θ_{p8}; Fig. 3) from the scleral mechanical testing data for each posterior scleral shell. This strategy uses a genetic optimization algorithm (differential evolution[47–49]) to generate a unique value for each of the 13 model parameters by simultaneously varying all 13 parameters until the FE-predicted displacements closely match the experimental deformations at five IOP levels simultaneously (7, 10, 20, 30, and 45 mm Hg).

Additional Measures of Scleral Stiffness

Two additional measures of scleral stiffness were derived from the 13 output parameters: the tangent modulus and the structural stiffness. Because of their high clinical relevance, these two stiffness measures are emphasized in the Results and Discussion sections.

Tangent Modulus. The model parameters c_3 and c_4 describe the stretch-induced stiffening of the collagen fibers, but do not represent a direct measure of scleral stiffness as a function of IOP. To capture scleral stiffness, the tangent modulus along the preferred fiber orientation was calculated and mapped. The tangent modulus is an estimate of local scleral material stiffness, varies with IOP, and is independent of geometry.[9]

Structural Stiffness. Clinical discussions concerning the observable mechanical behavior of the corneoscleral shell often confuse the difference between the biomechanical material properties of the tissue (the stiffness of the bulk material itself), its architecture (thickness), and the resultant net structural behavior. Although the material properties of the tissues are intrinsic to the material itself, the structural stiffness of the shell incorporates both the material properties and

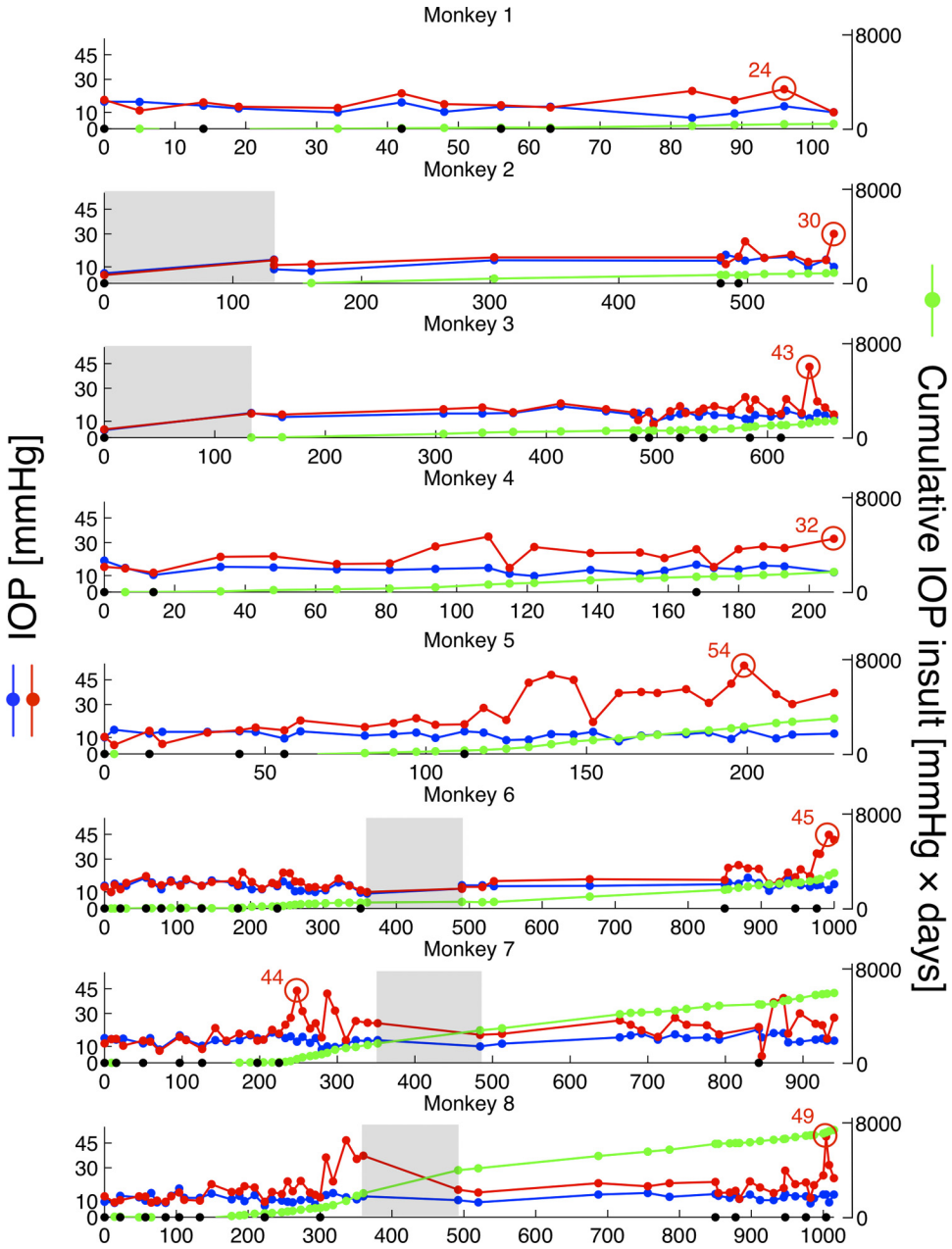

FIGURE 1. Postlaser-detected IOP in both eyes of each monkey (*blue*: normal eye; *red*: lasered eye). For each animal, time 0 corresponds to the first laser session, and the last day to the date of the monkey's death. *Black dots* along the *x*-axis signify each laser session. For each monkey, cumulative IOP insult (*green curve* in mm Hg × days; scale on the right) was defined as the difference in area under the IOP time curve between the lasered and the normal eyes. The animals were ordered such that monkey 1 received the lowest cumulative IOP insult, and monkey 8 the highest. Maximum detected IOP in each lasered eye is shown with a *red circle*. *Shaded area*: (August 30, 2005 to December 15, 2005) represents the period immediately after Hurricane Katrina, during which IOP could not be measured in monkeys 2, 3 and 6 to 8 (see the Limitations section of the Discussion). For these monkeys, an additional period of diminished frequency of IOP measurement occurred as the laboratory was becoming fully operational at Devers. Finally, note that the *x*-axis scale is not common to all animals and that chronic IOP elevations of different magnitude and duration were achieved in each lasered eye (also see Table 1).

geometry of a complex load-bearing structure into a composite measure of the structure's resistance to deformation. We defined the structural stiffness of the sclera as the local product of the scleral thickness and the tangent modulus to capture the mechanical behavior of the scleral shell as a structure in response to acute IOP elevations.

Data Analysis

Experimental Data. Regional thickness differences between the normal and glaucomatous eyes of each animal were compared to the regional thickness differences between bilaterally normal eyes of eight previously studied monkeys,[8] by using a multiple linear regression.

Posterior displacements between the two eyes of each monkey could not be directly compared, because all displacements were computed with respect to the position of the scleral clamp, which varied to a certain degree among eyes. However, the derived output measures (stress, strain, and structural stiffness) can be directly compared because they are unaffected by scleral clamp position.

Model Parameters. Tangent modulus and structural stiffness distributions for the eight adult normal eyes were compared to the previously reported data for four young and four old bilaterally normal monkeys at IOPs of 10, 30, and 45 mm Hg using the general estimating equation method as used in our previous report.[8]

Biomechanical Measures. Regional distributions of maximum principal stress, maximum principal strain, tangent modulus, and structural stiffness were compared between the normal and glaucomatous eyes of each monkey at IOPs of 10, 30, and 45 mm Hg by paired *t*-tests. Note that the regional data for these output measures (i.e., stress, strain, modulus, and stiffness) were not normally distributed, which violates the assumptions underlying *t*-tests. To address this, and as commonly performed using the central limit theorem, 3000 means were calculated for each parameter, each consisting of 300 randomly sampled values from the original distribution. The values of 300 and 3000 were chosen as the minimum values necessary for the *t*-statistic values to be unaffected by non-normality. These normally distributed means were then used in the *t*-tests to compare the parameters for

TABLE 1. Estimated Model Parameters from Inverse FE Simulations

Monkey	1		2		3		4	
CIOP insult, mm Hg × day	432		938		1479		1782	
Sex	F		F		F		F	
Age, y	17.9		22.7		23.0		19.3	
Weight, kg	8.1		11.3		13.3		8.6	
Eye	OS	OD	OS	OD	OS	OD	OS	OD
IOP Exp., mm Hg × day	1236	1668	7731	6793	10332	8853	4599	2816
Maximum IOP, mm Hg	17	24	30	17	43	19	34	19
IOP at sacrifice, mm Hg	10	10	30	10	14	12	32	12
c_1, kPa	1940	744	165	191	1607	1010	1669	482
c_3, kPa	15.1	0.90	27.9	35.7	5.84	24.0	1.41	3.30
c_4, –	876	1200	548	413	1938	1169	2517	913
k_1, –	2.15	2.28	0.49	1.66	4.99	1.32	1.30	1.64
k_2, –	3.54	2.46	2.25	1.93	1.58	4.03	1.41	0.64
Average nodal displacement fit error, μm	1.89	3.17	2.25	3.38	2.05	1.68	1.60	3.20

Monkey	5		6		7		8	
CIOP insult, mm Hg × day	3127		3128		6153		7714	
Sex	F		F		F		M	
Age, y	21.0		12.9		11.9		9.8	
Weight, kg	8.9		5.9		10.0		9.2	
Eye	OS	OD	OS	OD	OS	OD	OS	OD
IOP Exp., mm Hg × day	2693	5820	13545	16674	2693	5820	13545	16674
Maximum IOP, mm Hg	15	54	19	45	15	54	19	45
IOP at sacrifice, mm Hg	12	37	15	42	12	37	15	42
c_1, kPa	951	853	419	723	951	853	419	723
c_3, kPa	4.31	9.69	76.5	13.5	4.31	9.69	76.5	13.5
c_4, –	915	1209	413	1309	915	1209	413	1309
k_1, –	1.75	1.57	1.14	3.43	1.75	1.57	1.14	3.43
k_2, –	1.78	3.13	1.09	3.14	1.78	3.13	1.09	3.14
Average nodal displacement fit error, μm	2.23	2.20	2.52	2.73	2.23	2.20	2.52	2.73

Data are shown for both eyes of each monkey. The subject ID is shown above the column. The gray shaded column corresponds to the glaucomatous eye. Note that all eight other model parameters for each eye (the preferred fiber orientations) are shown in the last row of Figure 4. IOP exposure (IOP Exp) is defined as the area under the IOP time curve of each eye. The cumulative IOP (CIOP) insult is therefore the difference in IOP exposure between the eyes of each monkey.

normal and EG eyes. For each output measure (i.e., stress, strain, modulus, and stiffness), alterations due to chronic IOP elevation were deemed to be significant for that particular monkey when the *t* statistic from comparing the normal and glaucomatous eye of that monkey exceeded all *t* statistics computed from comparisons of bilaterally normal eyes of eight other monkeys.[8]

Finally, anisotropy parameters (i.e., preferred fiber orientation and fiber concentration factor) were compared between groups by paired *t*-tests in both the peripapillary and peripheral sclera.

RESULTS

Results Common to All Eyes

Scleral Thickness. Scleral thickness, experimentally measured at an IOP of 5 mm Hg at 20 locations and interpolated over each scleral shell, is shown in the first row of Figure 4 and in Figure 5 (averaged values). In all eyes, the peripapillary sclera was much thicker (276–498 μm on average in the normal eyes) than the peripheral sclera (157–252 μm on average in the normal eyes; $P < 0.0001$). Among those regions considered (inferior, inferonasal, nasal, superonasal, superior, superotemporal, temporal, and inferotemporal), the sclera was significantly thicker in the temporal region for all 16 eyes ($P < 0.001$).

FE Predictions. For each eye, good agreement was obtained between the FE-predicted and experimentally measured posterior displacements between 5 and 30 mm Hg (second and third rows of Fig. 4; Table 1; maximum averaged nodal error, 4.08 μm). Although not all cases are included in Figure 4, good agreement was also obtained for each IOP range (5–7, 5–10, 5–20, 5–30, and 5–45 mm Hg) and for all displacement components, suggesting that our constitutive model was able to accurately capture the complex 3-D deformations of the monkey peripapillary and posterior sclera after acute elevation of IOP.

Nonlinearity. For each eye, the sclera stiffened considerably as IOP increased, as demonstrated by the large increase in tangent modulus in Figure 6 (2.2–7.7-fold increase from 10 to 45 mm Hg in the peripapillary sclera from normal eyes), and also by the large increase in structural stiffness as IOP increased (Fig. 7). This phenomenon is also demonstrated by the nonlinear relationship between maximum principal strain and IOP (Fig. 8). Note that maximum principal strain values were consistently low in the normal eyes, as shown in blue in Figure 8, and varied between 0.32% and 1.49% on average in the peripapillary sclera at 45 mm Hg. Conversely, maximum principal stress increased linearly with IOP (Fig. 8) and was considerably higher than IOP (16 to 30 × IOP on average in the peripapillary sclera from normal eyes at all IOP levels).

Inhomogeneity. For each eye, the sclera was highly inhomogeneous as demonstrated by the regional variations in tangent modulus (Fig. 4, row 4). On average, the tangent modulus was higher in the peripheral sclera (17–60 MPa in the normal eyes) than in the peripapillary sclera (15–50 MPa in the normal eyes).

Anisotropy. The sclera was highly anisotropic in all eyes as demonstrated by the non-zero fiber concentration factors shown in Table 1 and Figure 2. The fiber concentration factor in the peripapillary sclera (k_2) was higher than that in the peripheral sclera (k_1) in 10 of the 16 eyes studied (Table 1). Maps of the predicted preferred fiber orientation for all eight

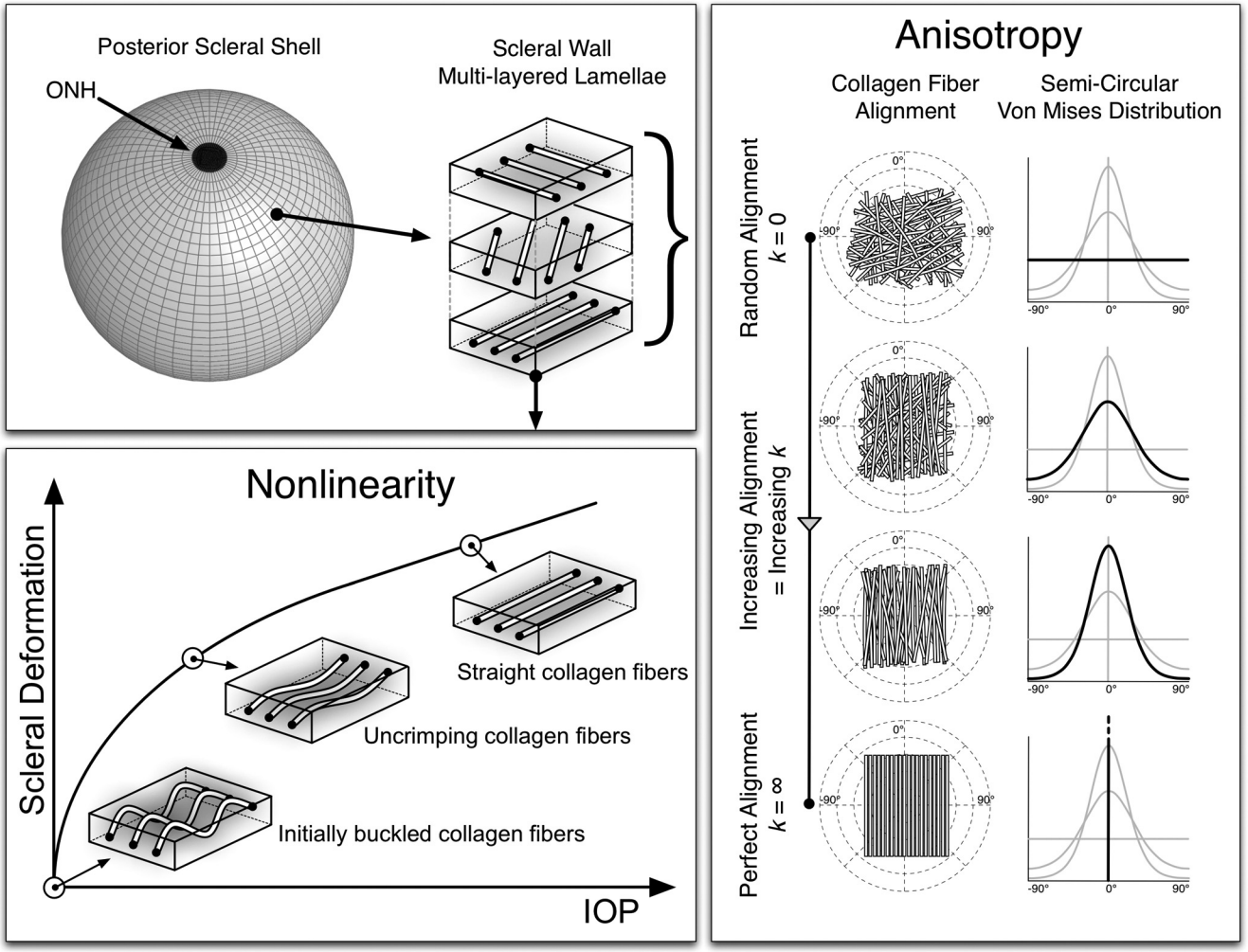

Figure 2. Nonlinearity and anisotropy are the two major biomechanical features that arise from the presence and organization of the scleral collagen fibers. These latter are assumed to run tangent to the scleral surface, according to previous histologic observations.[27] Both biomechanical features were incorporated mathematically into our constitutive model. Anisotropy: A semi-circular von Mises distribution is used to describe local collagen fiber alignment. As the fiber concentration factor k increases, collagen fibers become more aligned along the preferred fiber orientation (here, $\theta_p = 0°$). When $k = 0$, collagen fibers are randomly organized, resulting in equal stiffness in all directions (akin to some skin tissue[28]). This material symmetry is known as planar isotropy. When $k = \infty$, collagen fibers are all oriented along a unique preferred orientation, which creates high stiffness along θ_p and low stiffness perpendicular to θ_p (similar to tendons and ligaments[29]). This material symmetry is known as transverse isotropy, which is specific to planar fiber orientations. Nonlinearity: uncrimping of the collagen fibers induces scleral stiffening at the macroscopic level.[8,9,30–45] At low IOPs the collagen fibers are buckled, then uncrimp and straighten as they stretch in response to IOP elevations. As the collagen fibers uncrimp and straighten, they become stiffer, thereby limiting scleral deformation at high IOP values. Note that the parameters c_3 and c_4 govern the degree of nonlinearity of each scleral shell.

regions of each eye are shown in Figure 4, where ⊥ (white) indicates a preferred fiber orientation perpendicular to the scleral canal (meridional, $\theta_p = 0°$), and // (black) indicates a preferred fiber orientation tangent to the scleral canal (circumferential, $\theta_p = 90°$). Figure 9 shows the pooled distributions of the preferred fiber orientation for all 16 eyes in both the peripapillary and peripheral sclera. In general, the mean preferred fiber orientation for all tested eyes was tangent to the scleral canal in both scleral regions, but this effect was more pronounced in the peripapillary sclera.

Age-Related Changes in Scleral Biomechanics

We considered all eight normal eyes from this study as being part of one age group (adult, 17.3 ± 5.1 years). Note that the monkey lifespan is about one third the human lifespan.[51] We compared tangent modulus and structural stiffness distributions from the monkeys in this study to that of two other age groups (young, 1.5 ± 0.7 years; old, 22.9 ± 5.3 years) from our previous report.[8] Using the generalized estimating equation method, we found that the tangent modulus and structural stiffness in the peripapillary sclera significantly increased with age (Table 2). Using a multiple linear regression, we found that eyes from old monkeys were significantly thinner than eyes from adult monkeys ($P < 0.05$) but found no significant differences in thickness between eyes of young and adult monkeys ($P > 0.05$). Peripapillary scleral thickness averaged 389 ± 53 μm in young eyes,[8] 381 ± 47 μm in adult eyes (this study), and 349 ± 49 μm in old eyes.[8]

Changes in Scleral Biomechanics after Exposure to Chronic IOP Elevation

We observed no significant changes (exceeding the physiologic intereye difference of normal monkeys) in tangent mod-

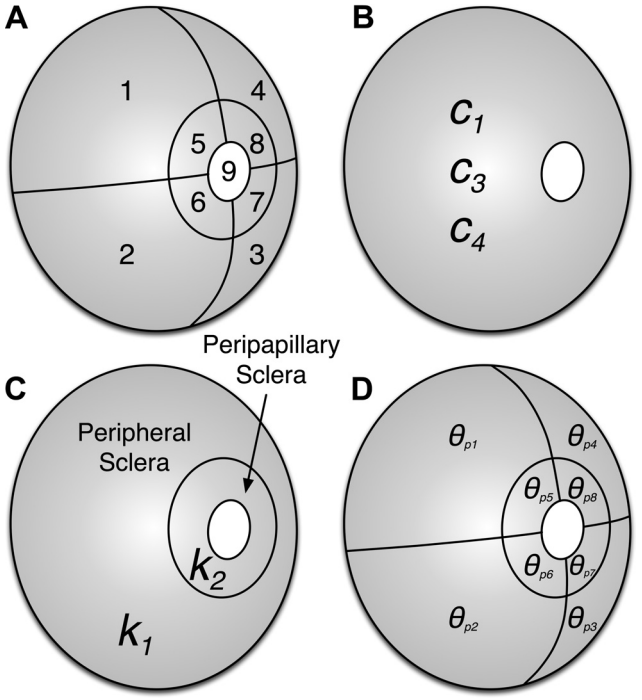

FIGURE 3. (**A**) Thirteen unique model parameters are estimated for each eye. Each reconstructed posterior scleral geometry was subdivided into nine regions: regions 1 to 4 represent the peripheral sclera, regions 5 to 8 the peripapillary sclera, and region 9 the ONH. (**B**) Three stiffness parameters were uniformly attributed to the entire scleral shell (c_1, first Mooney-Rivlin coefficient; c_3, exponential fiber stress coefficient; c_4, uncrimping rate of the collagen fibers). (**C**) Two structural parameters—fiber concentration factors k_1 and k_2—were attributed to the peripapillary and peripheral sclera respectively. (**D**) Eight other structural parameters—preferred fiber orientations θ_{p1} to θ_{p8}—were attributed to each of the eight scleral regions respectively. Note that the ONH was assumed linear isotropic with an elastic modulus fixed to 1 MPa for all normal and glaucomatous monkey eyes. This assumption is reasonable, as the ONH has been shown to have little impact on IOP-induced scleral deformations.[9,46]

ulus (Fig. 6) and structural stiffness (Fig. 7) between the normal and glaucomatous eyes of monkeys 2, 3, and 8.

We observed significant changes in tangent modulus (Fig. 6) and structural stiffness (Fig. 7) between the normal and glaucomatous eyes of monkeys 1, 4, 5, 6, and 7. The glaucomatous eye in monkey 1 exhibited a significant decrease in tangent modulus (10 mm Hg) and structural stiffness (10 and 30 mm Hg). Note that monkey 1 received the lowest cumulative IOP insult and these changes manifest at lower IOPs. The glaucomatous eyes in monkeys 4, 5, and 6 exhibited a significant increase in tangent modulus and structural stiffness at higher IOPs (30 and 45 mm Hg). Monkey 7 exhibited a significant increase in tangent modulus at 45 mm Hg in the peripheral sclera only.

We observed significant changes (exceeding the physiologic intereye difference of normal monkeys) in maximum principal strain in two of the eight monkeys (Fig. 8, 1 and 4) and in maximum principal stress in two of the eight monkeys (Fig. 8; 4 and 6).

We did not detect any changes in the fiber concentration factor ($P > 0.05$) or in the preferred fiber orientation ($P > 0.05$) in either the peripapillary or peripheral regions between the normal and glaucomatous eyes.

Finally, peripapillary and peripheral scleral thickness in both the normal and glaucomatous eyes of each monkey are shown in Figure 5. Although a trend toward scleral thinning was observed in the glaucomatous monkey eyes, overall and regional change in scleral thickness between glaucomatous and normal eyes was insignificant when compared to the physiologic intereye difference from eight normal monkey eyes ($P > 0.05$).

DISCUSSION

In this study, we characterized scleral biomechanical behavior in both eyes of eight adult monkeys in which one eye had been exposed to chronic, laser-induced IOP elevations of modest to substantial magnitude and duration. The following are the principal findings of this report.

All Eyes

When considered as a group of 16 monkey eyes without regard for experimental condition (normal versus EG) the eyes in this report behaved similarly to the eyes from bilaterally normal monkeys from a previous report,[8] as follows. First, the monkey posterior sclera is thicker in the peripapillary and temporal regions. Second, the monkey posterior sclera is a nonlinear, anisotropic, and inhomogeneous soft tissue. Third, concentrations of tangent modulus, structural stiffness, and maximum principal stress and strain were evident adjacent to the scleral canal in each eye. Fourth, maximum principal stress magnitude was substantially higher than IOP. Fifth, maximum principal strain magnitude was low. A detailed discussion of these results can be found in our previous report.[8]

Age-Related Changes in Scleral Biomechanics

Scleral biomechanical properties (i.e., tangent modulus and structural stiffness; Table 2) in the eight normal adult eyes (mean age, 17.3 ± 5.1 years) from this study fell between those from young (1.5 ± 0.7 years) and old (22.9 ± 5.3 years) monkeys from our previous aging study.[8] These findings separately confirm our initial report of age-related stiffening of the posterior sclera by establishing that adult eyes are stiffer than young ones but less stiff than old eyes. This result is likely to be related to increasing scleral cross-links with age[28,52]; details on this topic can be found in our previous report.[8]

We have reported a decrease in scleral thickness in old compared with young normal monkey eyes. In that study, we found that adult monkey sclera was not significantly thinner than young monkey sclera, but was significantly thicker than sclera from old monkey eyes. This finding is important because it suggests that the rate of scleral thinning, if present, may accelerate with age. Whether scleral thinning with age could accelerate the progression of glaucoma in elderly patients remains unclear. In monkeys, we observed a reduction in peripapillary scleral thickness of approximately 8.4% from adult to older eyes on average. In comparison, we observed an increase in tangent modulus of 37.4% (at 30 mm Hg). If both tangent modulus and thickness contribute similarly to the overall stiffness of the scleral shell (i.e., structural stiffness), then age-related changes in peripapillary scleral thickness will have a lesser impact on IOP-induced deformation than those of the tangent modulus. The relationship between glaucomatous susceptibility and scleral stiffness is likely to be complex, individual specific, and involve many interacting factors.

Changes in Scleral Biomechanics after Exposure to Chronic IOP Elevation

The major findings were as follows: First, significant changes in tangent modulus and structural stiffness were observed in some

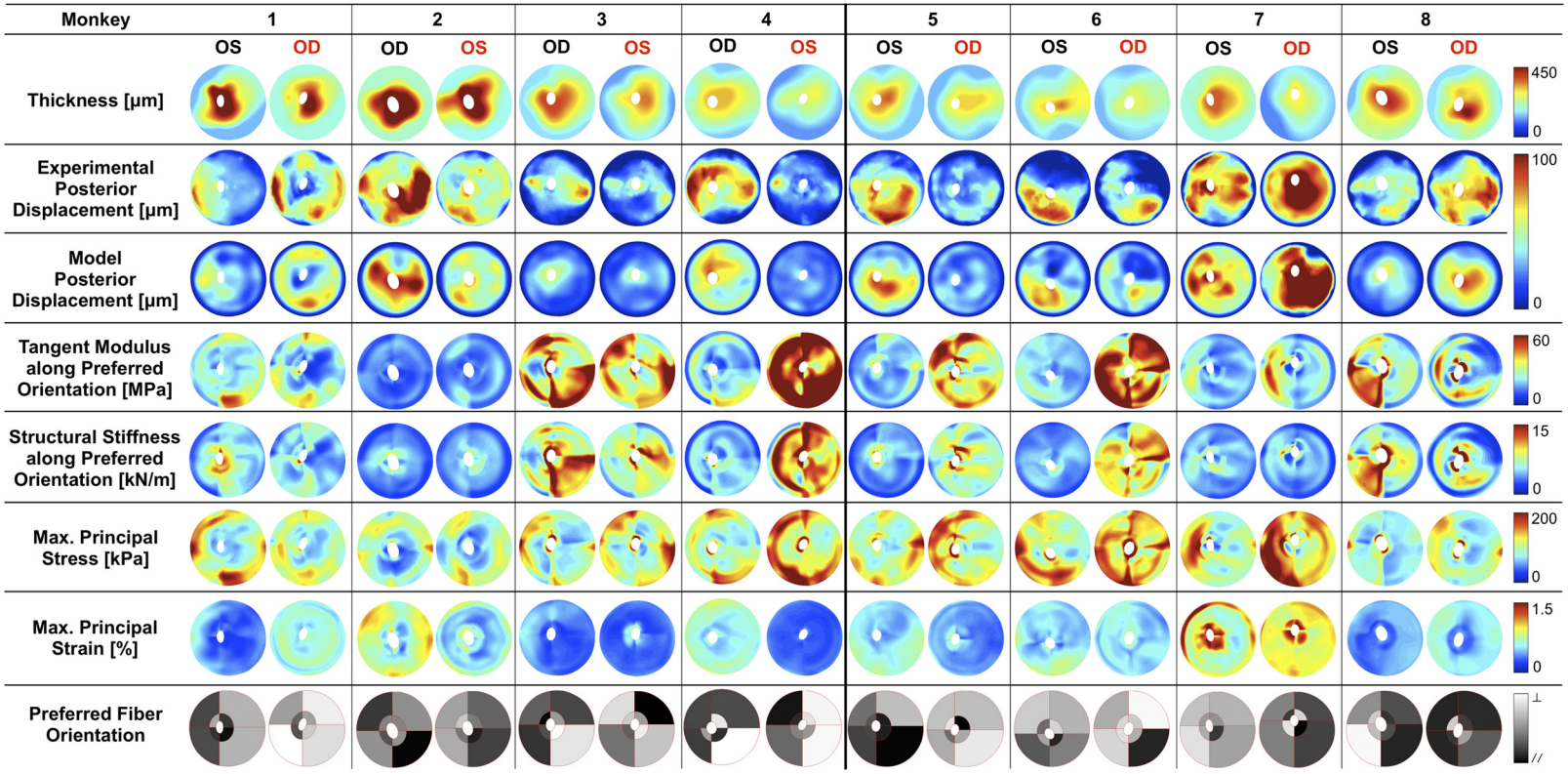

Figure 4. Experimental and modeling results for all posterior scleral shells as viewed from the back of the eye (superior is on *top*, all eyes are in OD configuration with temporal on the *right*). For each monkey, the glaucomatous eye is shown in *red* on the *right*. Scleral thickness was experimentally measured at an IOP of 5 mm Hg and interpolated to obtain continuous thickness maps. Tangent modulus, structural stiffness, and maximum principal stress and strain are shown for all eyes at a single IOP of 30 mm Hg. Good agreements were observed between the FE-computed and the experimentally measured posterior displacements (plotted for an IOP range, 5–30 mm Hg). Finally the preferred fiber orientation is shown for all eight regions of each eye, where // (*black*) corresponds to a collagen fiber organization tangent to the scleral canal (circumferential, $\theta_p = 0°$) and ⊥ (*white*) corresponds to a fiber organization that is perpendicular to the scleral canal (meridional, $\theta_p = 90°$).

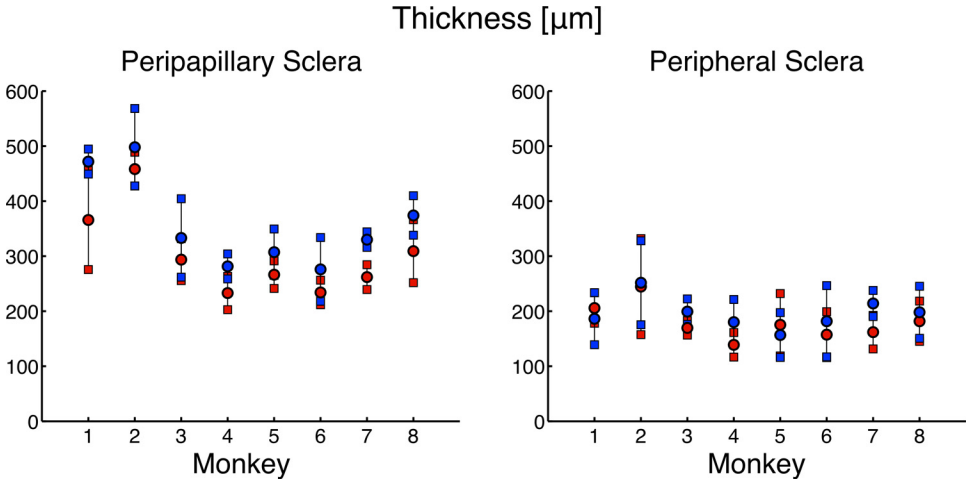

FIGURE 5. Peripapillary and peripheral scleral thickness (mean ± SD) in both normal (*blue*) and glaucomatous (*red*) eyes of each monkey. Overall, a decreasing trend in monkey scleral thickness was observed in glaucomatous eyes. However, this trend was not significant when compared with intereye thickness differences in the eight normal monkeys ($P > 0.05$).

monkeys between the normal eyes and those exposed to chronic IOP elevation. Second, changes in FE-based scleral anisotropy measures were not observed between normal and glaucomatous monkey eyes. Finally, although all glaucomatous eyes exhibited thinner peripapillary sclera than their contralateral normal eyes (Fig. 5), these differences did not achieve statistical significance.

We observed significant changes in scleral tangent modulus (Fig. 6) and structural stiffness (Fig. 7) between the normal and glaucomatous eyes of monkeys 1, 4, 5, 6, and 7. The glaucomatous eye in monkey 1 exhibited a smaller tangent modulus at 10 mm Hg (Fig. 6) and structural stiffness at 10 and 30 mm Hg (Fig. 7) than those of its contralateral normal. Burgoyne et al.[53] have reported hypercompliance of the ONH surface within 4 to 8 weeks of chronic IOP elevation in monkeys and suggested that weakening of the load-bearing structures of the eye (lamina cribrosa and peripapillary sclera) through connective tissue damage might be responsible for this phenomenon at the earliest stage of glaucomatous optic neuropathy. Moreover, a computational modeling study by Downs et al.[54] reported weakening of the lamina cribrosa structure at the earliest stage of glaucomatous optic neuropathy. It is interesting to note that weakening of the sclera was only present in the glaucomatous eye of monkey 1, the eye that received the smallest cumulative IOP insult (432 mm Hg × days) and had the lowest maximum measured IOP (24 mm Hg). It should also be noted that the decrease in tangent modulus in the glaucomatous eye of monkey 1 was only significant at low IOP (10 mm Hg).

In 1957, Roach and Burton[55] studied the roles of elastin and collagen in arteries. They found that elastin alone was responsible for resisting pressure-induced arterial deformations at low pressure and that collagen alone was responsible for resisting pressure-induced arterial deformations at high pressure. These results were recently confirmed by Fonck et al.[56] Based on these studies, it could be that only damage to elastin occurred in the glaucomatous eye of monkey 1, and this represents the earliest stage of scleral damage and/or remodeling in glaucomatous progression.

We observed a significant increase in scleral tangent modulus at IOPs of 30 and 45 mm Hg in both the peripapillary and peripheral regions in monkeys 4, 5, and 6, and a significant increase in scleral tangent modulus at 45 mm Hg in the peripapillary region in monkey 7 (Fig. 6). The glaucomatous eyes in monkeys 4, 5, and 6 also exhibited larger structural stiffness in the peripapillary sclera at IOPs of 30 and 45 mm Hg (Fig. 7). These findings suggest that at higher levels of cumulative IOP insult, the posterior sclera stiffens through extracellular matrix remodeling. This finding is consistent with that in our previous uniaxial study of scleral biomechanics in glaucomatous monkey eyes[11] and may be a protective mechanism that limits scleral canal expansion and related deformation of the ONH at elevated IOPs. Zeimer and Ogura[57] reported that human ONHs became more rigid with severe glaucoma, a result that is consistent with this hypothesis. Roach and Burton[55] also demonstrated that collagen alone was responsible for limiting arterial deformations at high pressure, which suggests that the observed increase in tangent modulus in glaucomatous eyes at high IOPs may be due primarily to collagen remodeling.

Even though tangent modulus changes occurred in five monkeys (1, 4, 5, 6, and 7), significant changes in maximum principal strains (monkeys 1 and 4) and maximum principal stress (monkeys 4 and 6, in the peripapillary sclera only) were each observed in only two monkeys. This result suggests that overall changes in scleral thickness (generally lower in the glaucoma eyes) and tangent modulus (generally higher in the glaucoma eyes) at this stage of damage interact to maintain the stress and strain ranges typical of sclera in normal eyes.

In this study, we observed no significant changes in either scleral tangent modulus (Fig. 6) or structural stiffness (Fig. 7) between the normal and glaucomatous eyes in three monkeys (2, 3, and 8). Since monkey 8 received the highest cumulative IOP insult (7714 mm Hg × days), we would have expected to observe the largest changes in the glaucomatous eye of this monkey. Of note, at IOPs of 30 and 45 mm Hg, the normal eyes of monkeys 3 and 8 had the two highest mean tangent moduli and structural stiffnesses in the peripapillary sclera. Assuming that before IOP insult, the glaucomatous eyes in monkeys 3 and 8 were as stiff as their contralateral normals, these results suggest that stiffer scleral shells may be less prone to biomechanical changes when exposed to chronic IOP elevation, presumably because they are more resistant to IOP-induced strain.

Several studies have reported that mechanical strain applied to scleral fibroblasts can trigger the release of MMPs and TIMPs,[58–61] which can then lead to remodeling of the scleral extracellular matrix. IOP-induced scleral shell expansion increases scleral strain in all eyes, but in eyes with the stiffest sclera, these increases may be too small to elicit a fibroblast response. Note that mean strain levels at 45 mm Hg in monkeys 3 and 8 were 0.30% and 0.32% respectively, which were smaller than all the reported values in the aforementioned in vitro studies on scleral fibroblast response to strain (a minimum of 0.45%[58]).

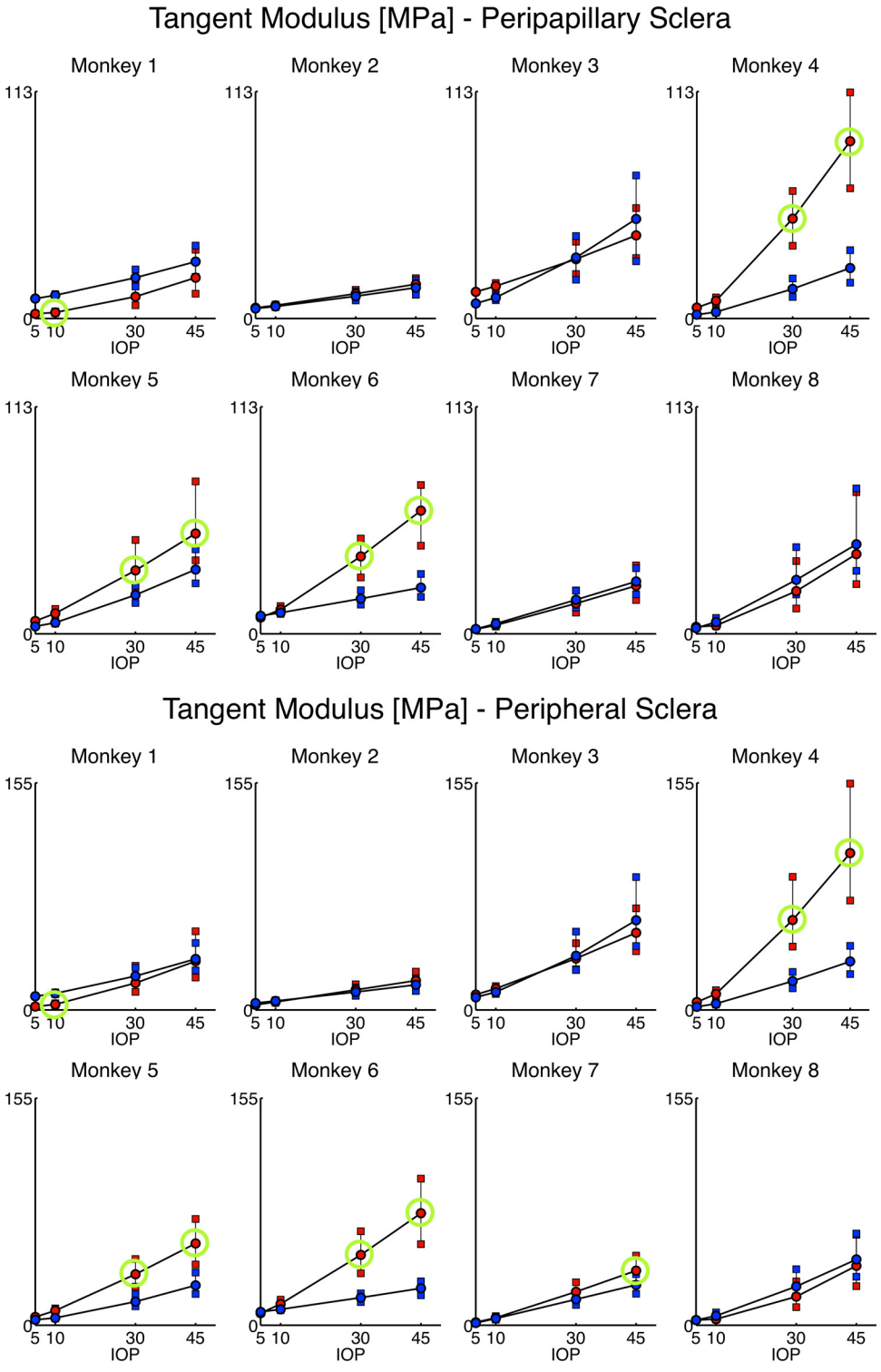

Figure 6. Tangent modulus in both eyes (*blue*: normal, *red*: glaucomatous) and for both the peripapillary (*top*) and peripheral (*bottom*) scleral regions of each monkey as a function of IOP. Error bars show the 25th, 50th, and 75th percentiles. *Green circle*: a significant difference between the normal and glaucomatous eye that also exceeds the intereye differences from eight normal monkeys.

In the case of the third monkey, which demonstrated no change in tangent modulus or structural stiffness (monkey 2), the normal eye had the most scleral thickness (Fig. 5), and lowest tangent modulus (Fig. 6) among all normal eyes. Its mean structural stiffness was therefore comparable with the mean structural stiffness of all normal eyes. These data suggest that mean structural stiffness may not always predict which eyes will undergo IOP-induced scleral remodeling and that scleral thickness may also be an important contributor in predicting which eyes will be less sensitive to biomechanical change.[5,46]

In this study, we did not observe significant differences in predicted scleral anisotropy (preferred fiber orientation and fiber concentration factor) between normal and glaucomatous monkey eyes. The preservation of anisotropy was recently reported for the remodeled monkey lamina cribrosa in EG,[15] suggesting that remodeling of the peripapillary and posterior sclera must be accompanied by changes in elastin/collagen content and/or fiber diameter, but not fiber reorientation. This is consistent with the work of Quigley et al.,[62] who reported glaucomatous changes in collagen and elastin content and

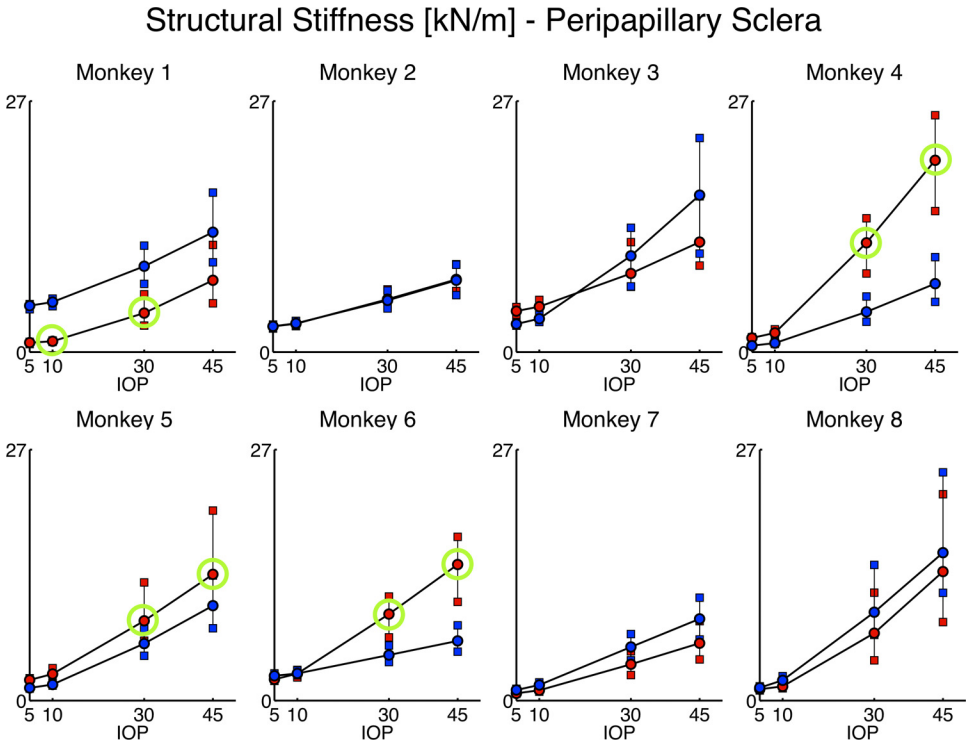

FIGURE 7. Structural stiffness (thickness × tangent modulus) in the peripapillary sclera in both eyes (*blue*: normal; *red*: glaucomatous) of each monkey as a function of IOP. Error bars show the 25th, 50th, and 75th percentiles. *Green circle*: a significant difference between the normal and glaucomatous eye (when the *t*-statistic is greater than the intereye differences in the eight normal monkeys).

collagen fiber diameter in the peripapillary sclera in human and monkey eyes.

Although we did observe a trend toward scleral thinning in the glaucomatous eyes, this difference did not exceed the physiologic intereye differences in the eight normal monkeys. Using traditional histology, we previously reported significant thinning of the posterior[10] and peripapillary sclera[13,14] in monkey eyes subjected to chronic IOP elevation. Scleral morphologic changes should be assessed in future studies to understand whether scleral thinning due to chronic IOP elevation is a consequence of strain-induced fluid exudation, tissue loss, or a combination of the two.

Overall, our data suggest that a stiffer scleral shell is biomechanically beneficial and is less apt to remodel in response to elevated IOP. In normal eyes, we suggest that the sclera shields the ONH from biomechanical insult by resisting large overall deformation (through uncrimping and stiffening of the collagen fibers: nonlinearity) and large scleral canal expansion (through the presence of a circumferential peripapillary ring of collagen fibers: anisotropy).[3,4,8] We hypothesize that the scleral stiffening in response to moderate exposure to chronic IOP elevations shown herein is an effort to maintain the biomechanical homeostasis of the scleral shell and indirectly, the ONH. As such, this response could act to slow glaucomatous progression in eyes with higher IOPs and/or more compliant scleral shells. Surprisingly, the argument that a stiff scleral shell shields the ONH from glaucomatous damage seems to contradict the facts that (1) the sclera stiffens with age.[8] and (2) the elderly are more susceptible to glaucoma.[63] To reconcile all these observations, it should be noted that collagen fibers become brittle with age[28] and therefore it is plausible to suggest that scleral stiffening with age is an unhealthy mechanism as opposed to scleral stiffening because of the remodeling seen in this study. In addition, there are other factors that are likely to contribute to glaucomatous damage, including blood flow and cellular reactivity, and these factors change with age as well. We also caution the reader that stiffness is a broad term, and reporting a single stiffness value for the sclera does not represent its biomechanical response well. Scleral stiffness is a function of IOP (nonlinearity), orientation (anisotropy), and location (heterogeneity). This complexity should be taken into account when evaluating the contribution of scleral biomechanics to glaucoma pathogenesis.

Limitations

Several limitations should be recognized when viewing this work. Although the general limitations of the method have been discussed at length in our previous reports,[3,8,9] we will briefly revisit them and then discuss those inherent to this study.

First, IOP was measured in both eyes of each monkey over time (Fig. 1), but we did not characterize the diurnal and nocturnal IOP fluctuations that are known to exist in monkeys. Diurnal IOP fluctuations have been shown to be large in monkeys, especially in glaucomatous eyes, in which they are highly individual-specific and can exceed 10 mm Hg.[64] Therefore, our definition of cumulative IOP insult (change in area under the IOP/time curve) should be regarded with caution and was used here only to provide a rough estimate of the cumulative insult from IOP. An implantable telemetric IOP transducer is currently being developed for monkeys that should allow for continuous measurements of diurnal and nocturnal IOP fluctuations and more accurate characterization of IOP insult (Downs JC, et al. *IOVS* 2008;49: ARVO E-Abstract 2043).

Second, because the sclera is approximately 90% collagen by weight,[65] we assumed that collagen is the primary fibrous element[66] of this tissue. We lumped all other tissue constituents into the ground substance matrix, a common practice in soft-tissue FE modeling.[4,30,67–71] Because our study suggests that both elastin and collagen play important roles in glaucomatous damage, further experimental and theoretical work is needed to address how these components separately contribute to scleral biomechanics.

Third, we did not characterize scleral biomechanics between 0 and 5 mm Hg in the tested eyes, because the scleral

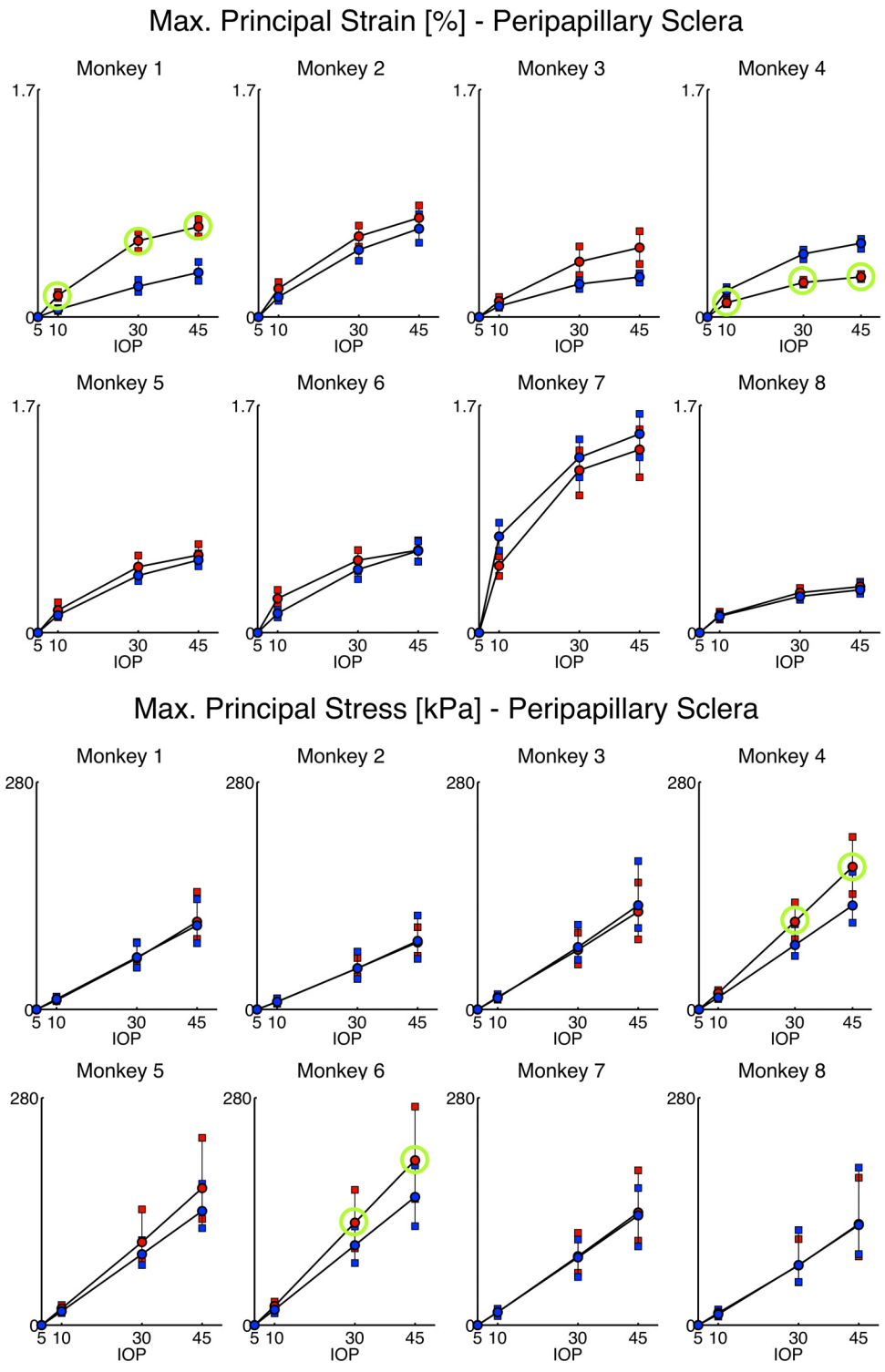

FIGURE 8. Maximum principal strain (*top*) and stress (*bottom*) in the peripapillary sclera in both eyes (*blue*: normal, r*ed*: glaucomatous) of each monkey as a function of IOP. Error bars show the 25th, 50th, and 75th percentiles. *Green circle*: represents a significant difference between the normal and glaucomatous eye (when the *t*-statistic is greater than the inter-eye differences in the eight normal monkeys). Note that the maximum principal strain is a nonlinear function of IOP and the maximum principal stress is a linear function of IOP.

shells required an IOP of approximately 4 mm Hg to sustain their shape. IOPs in the range of 0 to 5 mm Hg are rarely measured in monkey eyes, and so ignoring the initial IOP loading should not compromise the clinical importance of our results. We are developing methods that will allow the initial scleral stress and strain that exist in the tissues at 5 mm Hg to be estimated and included in future studies.

Fourth, the ONH tissues were assumed to be linearly elastic, with a common elastic modulus of 1 MPa assigned to the ONH region for both normal and glaucomatous monkey eyes. Our previous sensitivity study showed that ONH elastic moduli in the range of 0.1 to 5 MPa did not affect the results of our scleral biomechanical property fitting[9]; hence, our assumption should not affect the results presented herein.

Fifth, within our models the ONH was represented as an elliptical cylinder, with its external boundary located at the outer aspect of the dural sheath insertion (as measured with the 3-D digitizer) and therefore included regions of the immediate peripapillary sclera and scleral flange. As a result of this anatomic convention, we could not estimate biomechanical properties for that region of the sclera that lies immediately under the dural sheath insertion.

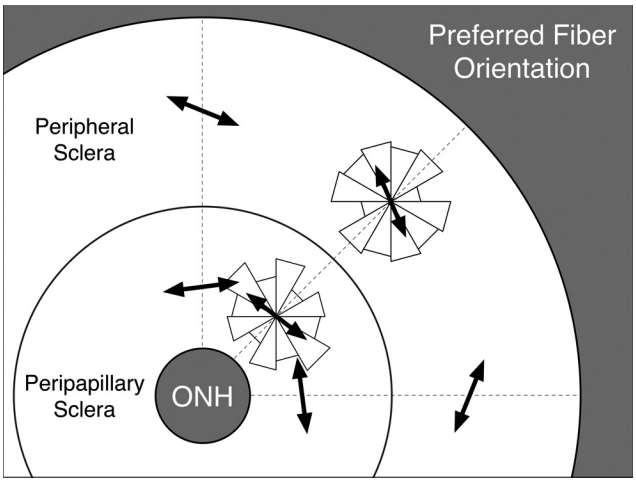

FIGURE 9. Pooled distributions (all eyes) of the preferred fiber orientation for both the peripapillary and peripheral scleral regions are shown as two symmetric rose diagrams with 30° segment, in which larger *triangles* indicate the most commonly predicted orientations. Mean preferred fiber orientations (*arrows*) were calculated from the distributions using circular statistics.[50] The result suggests a circumferential organization of the collagen fibers around the scleral canal in both the peripapillary (stronger) and the peripheral (weaker) sclera.

Sixth, we divided each reconstructed scleral shell into eight regions to assess regional variations in predicted collagen fiber orientation (θ_{p1}-θ_{p8}). This division was made because a preliminary study confirmed that a combination of eight regions and 13 model parameters was the minimum requirement to obtain good agreement between the FE-predicted and experimentally measured displacements (Fig. 4), while also ensuring a unique set of model parameters. Future studies will include a more rigorous assessment of regional variability.

Seventh, all experiments were conducted at room temperature (22°C) because the incorporation of a heated saline chamber at 37°C proved incompatible with the speckle interferometry sensor we used. Because all experiments were consistently performed at the same temperature, all hypotheses tested regarding the changes in scleral biomechanics should be valid.

Eighth, collagen fiber alignment was not measured directly, but was predicted using the models' fits to experimental scleral deformations (Fig. 4). Because of the relatively coarse discretization of the regions (discussed above) we could only report an overall approximation of the preferred collagen fiber orientation within each region. Future inclusion of experimental measures of collagen fiber orientation as input parameters, as currently being measured with small-angle light-scattering (Girard MJ, et al. *IOVS* 2010;51:ARVO E-Abstract 2128), will allow for finer regional discretization for the remaining fitted parameters and improve our characterization of scleral anisotropy.

Finally, seven of the eight monkeys (monkeys 2–8) began this study while the investigators laboratories were still located at the LSU Eye Center in New Orleans, and were unavailable for study for more than 3 months after Hurricane Katrina. Monkeys 2 and 3 and 6 to 8, however, had already undergone initial laser, and so the accuracy of their cumulative IOP exposure calculations is affected by the lack of IOP data between 30 August and 15 December 2005, (Fig. 1, shaded area) and the diminished frequency of testing after their arrival at Devers. In addition, these monkeys (2, 3, and 6 to 8) were examined only sporadically until the laboratory at Devers became fully operational. At the time of the hurricane, monkeys 4 and 5 had not yet been lasered, and so the frequency of IOP measurement and assessment of pre- and postlaser cumulative IOP exposure in these animals was unaffected by the hurricane. Monkey 1 was purchased at Devers and was altogether unaffected by these events.

Summary

In summary, new experimental and computational methodologies[3,9] were used in this study to characterize scleral biomechanics in normal and glaucomatous monkey eyes. These methods have broad applicability and can be applied to other thin, soft tissues with multidirectional collagen fibers. The long-term goal of this work is to establish the pathophysiologic mechanisms linking connective tissue stress and strain within the peripapillary sclera and lamina cribrosa to retinal ganglion cell axon damage and death. Given the important role of scleral biomechanics in determining the biomechanics of the ONH, new strategies for the clinical visualization and measurement of peripapillary and posterior scleral biomechanics are needed.

Overall, our results suggest that significant changes in the biomechanical behavior of the sclera are associated with exposure to chronic IOP elevations. These changes are complex and individual-specific and are likely to be the result of scleral extracellular matrix remodeling. Our findings suggest that (1) scleras with initially large tangent modulus or thickness are more resistant to IOP-induced biomechanical changes, (2) a decrease in tangent modulus (possibly due to elastin damage) occurs at the earliest stage of glaucoma, (3) an increase in tangent modulus (possibly associated with collagen changes) occurs at moderate stages of glaucoma, and (4) collagen fiber reorientation does not occur on a large scale in glaucomatous

TABLE 2. Median of Tangent Modulus and Structural Stiffness Distributions in the Peripapillary Sclera

	Young			Adult			Old		
	10	**30**	**45**	**10**	**30**	**45**	**10**	**30**	**45**
Age (mean ± SD), y		1.5 ± 0.7			17.3 ± 5.1			22.9 ± 5.3	
Tangent modulus, MPa	3.6*	8.3*	12.5*	6.5	17.9	26.6	8.8†	24.6‡	40.1‡
Structural stiffness, kN/m	1.4†	3.4‡	5.1‡	2.8	6.5	9.6	3.3	8.8†	14.4†

Data are the median (50th percentile) for each IOP (10, 30, and 45 mm Hg). Young and old monkey groups were used in a previous study on scleral biomechanics in the aging monkey eye. Distributions from young and old monkeys were compared to those of adult monkeys by using the generalized estimating equation method. Significant differences between the young and adult groups and between the adult and old groups were found in all but one comparison.

* $P < 0.001$.

† $P < 0.05$.

‡ $P < 0.01$.

eyes. The sclera drives the levels of stress and strain transmitted to the ONH, so changes in scleral biomechanical behavior will inevitably perturb the biomechanics of the ONH.[7] Scleral remodeling induced by exposure to chronic IOP elevations may provide a protective mechanism for the contained ONH and act to keep stress and strain levels within the normal range, but future work is necessary to establish the link between scleral/ONH biomechanics and glaucomatous vision loss.[72–74]

Acknowledgments

The authors thank Juan Reynaud, Jonathan Grimm, Wenxia Wang, and Stuart Gardiner for their contributions to this work.

References

1. Resnikoff S, Pascolini D, Etya'ale D, et al. Global data on visual impairment in the year 2002. *Bull World Health Organ.* 2004;82:844–851.
2. Foster A, Resnikoff S. The impact of Vision 2020 on global blindness. *Eye.* 2005;19:1133–1135.
3. Girard MJ, Downs JC, Burgoyne CF, Suh JK. Peripapillary and posterior scleral mechanics-part I: development of an anisotropic hyperelastic constitutive model. *J Biomech Eng.* 2009;131:051011.
4. Grytz R, Meschke G, Jonas JB. The collagen fibril architecture in the lamina cribrosa and peripapillary sclera predicted by a computational remodeling approach. *Biomech Model Mechanobiol.* Published online July 14, 2010.
5. Sigal IA, Flanagan JG, Tertinegg I, Ethier CR. Finite element modeling of optic nerve head biomechanics. *Invest Ophthalmol Vis Sci.* 2004;45:4378–4387.
6. Norman RE, Flanagan JG, Sigal IA, Rausch SM, Tertinegg I, Ethier CR. Finite element modeling of the human sclera: Influence on optic nerve head biomechanics and connections with glaucoma. *Exp Eye Res.* Published online September 29, 2010.
7. Sigal IA, Yang H, Roberts MD, Burgoyne CF, Downs JC. IOP-induced lamina cribrosa displacement and scleral canal expansion: an analysis of factor interactions using parameterized eye-specific models. *Invest Ophthalmol Vis Sci.* 2011;52:1896–1907.
8. Girard MJ, Suh JK, Bottlang M, Burgoyne CF, Downs JC. Scleral biomechanics in the aging monkey eye. *Invest Ophthalmol Vis Sci.* 2009;50:5226–5237.
9. Girard MJ, Downs JC, Bottlang M, Burgoyne CF, Suh JK. Peripapillary and posterior scleral mechanics. Part II: experimental and inverse finite element characterization. *J Biomech Eng.* 2009;131:051012.
10. Downs JC, Ensor ME, Bellezza AJ, Thompson HW, Hart RT, Burgoyne CF. Posterior scleral thickness in perfusion-fixed normal and early-glaucoma monkey eyes. *Invest Ophthalmol Vis Sci.* 2001;42:3202–3208.
11. Downs JC, Suh JK, Thomas KA, Bellezza AJ, Hart RT, Burgoyne CF. Viscoelastic material properties of the peripapillary sclera in normal and early-glaucoma monkey eyes. *Invest Ophthalmol Vis Sci.* 2005;46:540–546.
12. Downs JC, Yang H, Girkin C, et al. Three-dimensional histomorphometry of the normal and early glaucomatous monkey optic nerve head: neural canal and subarachnoid space architecture. *Invest Ophthalmol Vis Sci.* 2007;48:3195–3208.
13. Yang H, Downs JC, Bellezza A, Thompson H, Burgoyne CF. 3-D histomorphometry of the normal and early glaucomatous monkey optic nerve head: prelaminar neural tissues and cupping. *Invest Ophthalmol Vis Sci.* 2007;48:5068–5084.
14. Yang H, Downs JC, Girkin C, et al. 3-D histomorphometry of the normal and early glaucomatous monkey optic nerve head: lamina cribrosa and peripapillary scleral position and thickness. *Invest Ophthalmol Vis Sci.* 2007;48:4597–4607.
15. Roberts MD, Grau V, Grimm J, et al. Remodeling of the connective tissue microarchitecture of the lamina cribrosa in early experimental glaucoma. *Invest Ophthalmol Vis Sci.* 2009;50:681–690.
16. Burgoyne CF, Downs JC, Bellezza AJ, Hart RT. Three-dimensional reconstruction of normal and early glaucoma monkey optic nerve head connective tissues. *Invest Ophthalmol Vis Sci.* 2004;45:4388–4399.
17. Bellezza AJ, Rintalan CJ, Thompson HW, Downs JC, Hart RT, Burgoyne CF. Anterior scleral canal geometry in pressurised (IOP 10) and non-pressurised (IOP 0) normal monkey eyes. *Br J Ophthalmol* 2003;87:1284–1290.
18. Bellezza AJ, Rintalan CJ, Thompson HW, Downs JC, Hart RT, Burgoyne CF. Deformation of the lamina cribrosa and anterior scleral canal wall in early experimental glaucoma. *Invest Ophthalmol Vis Sci.* 2003;44:623–637.
19. Yang H, Downs JC, Sigal IA, Roberts MD, Thompson H, Burgoyne CF. Deformation of the normal monkey optic nerve head connective tissue after acute IOP elevation within 3-D histomorphometric reconstructions. *Invest Ophthalmol Vis Sci.* 2009;50:5785–5799.
20. Downs JC, Roberts MD, Sigal IA. Glaucomatous cupping of the lamina cribrosa: a review of the evidence for active progressive remodeling as a mechanism. *Exp Eye Res.* Epub ahead of print; doi:10.1016/j.exer.2010.08.004; 2010 Aug 11.
21. Burgoyne CF, Downs JC, Bellezza AJ, Suh JK, Hart RT. The optic nerve head as a biomechanical structure: a new paradigm for understanding the role of IOP-related stress and strain in the pathophysiology of glaucomatous optic nerve head damage. *Prog Retin Eye Res.* 2005;24:39–73.
22. Burgoyne CF. A biomechanical paradigm for axonal insult within the optic nerve head in aging and glaucoma. *Exp Eye Res.* Published online September 20, 2010.
23. Chauhan BC, Hutchison DM, Artes PH, et al. Optic disc progression in glaucoma: comparison of confocal scanning laser tomography to optic disc photographs in a prospective study. *Invest Ophthalmol Vis Sci.* 2009;50:1682–1691.
24. Yang H, Thompson H, Roberts MD, Sigal IA, Downs JC, Burgoyne CF. Deformation of the early glaucomatous monkey optic nerve head connective tissue after acute IOP elevation in 3-D histomorphometric reconstructions. *Invest Ophthalmol Vis Sci.* 2011;52:345–363.
25. Erne OK, Reid JB, Ehmke LW, Sommers MB, Madey SM, Bottlang M. Depth-dependent strain of patellofemoral articular cartilage in unconfined compression. *J Biomech.* 2005;38:667–672.
26. Kessler O, Lacatusu E, Sommers MB, Mayr E, Bottlang M. Malrotation in total knee arthroplasty: effect on tibial cortex strain captured by laser-based strain acquisition. *Clin Biomech (Bristol, Avon).* 2006;21:603–609.
27. Watson PG, Young RD. Scleral structure, organisation and disease. A review. *Exp Eye Res.* 2004;78:609–623.
28. Bailey AJ, Paul RG, Knott L. Mechanisms of maturation and ageing of collagen. *Mech Ageing Dev.* 1998;106:1–56.
29. Weiss JA, Gardiner JC. Computational modeling of ligament mechanics. *Crit Rev Biomed Eng.* 2001;29:303–371.
30. Grytz R, Meschke G. Constitutive modeling of crimped collagen fibrils in soft tissues. *J Mech Behav Biomed Mater.* 2009;2:522–533.
31. Girard MJ, Downs JC, Burgoyne CF, Suh JK. Experimental surface strain mapping of porcine peripapillary sclera due to elevations of intraocular pressure. *J Biomech Eng.* 2008;130:041017.
32. Spoerl E, Boehm AG, Pillunat LE. The influence of various substances on the biomechanical behavior of lamina cribrosa and peripapillary sclera. *Invest Ophthalmol Vis Sci.* 2005;46:1286–1290.
33. Siegwart JT Jr, Norton TT. Regulation of the mechanical properties of tree shrew sclera by the visual environment. *Vision Res.* 1999;39:387–407.
34. Curtin BJ. Physiopathologic aspects of scleral stress-strain. *Trans Am Ophthalmol Soc.* 1969;67:417–461.
35. Schultz DS, Lotz JC, Lee SM, Trinidad ML, Stewart JM. Structural factors that mediate scleral stiffness. *Invest Ophthalmol Vis Sci.* 2008;49:4232–4236.
36. Woo SL, Kobayashi AS, Schlegel WA, Lawrence C. Nonlinear material properties of intact cornea and sclera. *Exp Eye Res.* 1972;14:29–39.
37. Phillips JR, McBrien NA. Form deprivation myopia: elastic properties of sclera. *Ophthalmic Physiol Opt.* 1995;15:357–362.
38. Wollensak G, Spoerl E. Collagen crosslinking of human and porcine sclera. *J Cataract Refract Surg.* 2004;30:689–695.
39. Olesen CG, Tertinegg I, Eilaghi A, et al. Measuring the biaxial stress-strain characteristics of the human sclera. *Proceedings of the*

ASME Summer Bioengineering Conference. New York: ASME Press; 2007.

40. Weiyi C, Wang X, Wang C, Tao L, Li X, Zhang Q. An experimental study on collagen content and biomechanical properties of sclera after posterior sclera reinforcement. *Clin Biomech (Bristol, Avon).* 2008;23(suppl 1):S17–S30.
41. Thornton IL, Dupps WJ, Roy AS, Krueger RR. Biomechanical effects of intraocular pressure elevation on optic nerve/lamina cribrosa before and after peripapillary scleral collagen cross-linking. *Invest Ophthalmol Vis Sci.* 2009;50:1227–1233.
42. Myers KM, Cone FE, Quigley HA, Gelman S, Pease ME, Nguyen TD. The in vitro inflation response of mouse sclera. *Exp Eye Res.* 2010;91:866–875.
43. Myers KM, Coudrillier B, Boyce BL, Nguyen TD. The inflation response of the posterior bovine sclera. *Acta Biomater.* 2010;6:4327–4335.
44. Eilaghi A, Flanagan JG, Tertinegg I, Simmons CA, Wayne Brodland G, Ross Ethier C. Biaxial mechanical testing of human sclera. *J Biomech.* 2010;43:1696–1701.
45. Elsheikh A, Geraghty B, Alhasso D, Knappett J, Campanelli M, Rama P. Regional variation in the biomechanical properties of the human sclera. *Exp Eye Res.* 2010;90:624–633.
46. Sigal IA, Flanagan JG, Ethier CR. Factors influencing optic nerve head biomechanics. *Invest Ophthalmol Vis Sci.* 2005;46:4189–4199.
47. Olberding JE, Suh J-KF. A dual optimization method for the material parameter identification of a biphasic poroviscoelastic hydrogel: potential application to hypercompliant soft tissues. *J Biomech* 2006;39:2468–2475.
48. Price KV, Storn RM, Lampinen JA. *Differential Evolution: A Practical Approach to Global Optimization.* Berlin, Germany Springer; 2005.
49. Girard M, Suh JK, Hart RT, Burgoyne CF, Downs JC. Effects of storage time on the mechanical properties of rabbit peripapillary sclera after enucleation. *Curr Eye Res.* 2007;32:465–470.
50. Fisher NI. *Statistical Analysis of Circular Data.* Cambridge, UK: Cambridge University Press; 1993.
51. Tigges J, Gordon TP, McClure HM, Hall EC, Peters A. Survival rate and life span of rhesus monkeys at the Yerkes regional primate research center. *Am J Primatol.* 1988;15:263–273.
52. Bailey AJ. Structure, function and ageing of the collagens of the eye. *Eye.* 1987;1:175–183.
53. Burgoyne CF, Quigley HA, Thompson HW, Vitale S, Varma R. Early changes in optic disc compliance and surface position in experimental glaucoma. *Ophthalmology.* 1995;102:1800–1809.
54. Downs JC, Roberts MD, Burgoyne CF, Hart RT. Finite element modeling of the lamina cribrosa microarchitecture in the normal and early glaucoma optic nerve head *Proceedings of the ASME Summer Bioengineering Conference.* New York: ASME Press; 2007.
55. Roach MR, Burton AC. The reason for the shape of the distensibility curves of arteries. *Can J Biochem Physiol.* 1957;35:681–690.
56. Fonck E, Prod'hom G, Roy S, Augsburger L, Rufenacht DA, Stergiopulos N. Effect of elastin degradation on carotid wall mechanics as assessed by a constituent-based biomechanical model. *Am J Physiol Heart Circ Physiol.* 2007;292:H2754–H2763.
57. Zeimer RC, Ogura Y. The relation between glaucomatous damage and optic nerve head mechanical compliance. *Arch Ophthalmol.* 1989;107:1232–1234.
58. Yamaoka A, Matsuo T, Shiraga F, Ohtsuki H. TIMP-1 production by human scleral fibroblast decreases in response to cyclic mechanical stretching. *Ophthalmic Res.* 2001;33:98–101.
59. Cui W, Bryant MR, Sweet PM, McDonnell PJ. Changes in gene expression in response to mechanical strain in human scleral fibroblasts. *Exp Eye Res.* 2004;78:275–284.
60. Shelton L, Rada JS. Effects of cyclic mechanical stretch on extracellular matrix synthesis by human scleral fibroblasts. *Exp Eye Res.* 2007;84:314–322.
61. Fujikura H, Seko Y, Tokoro T, Mochizuki M, Shimokawa H. Involvement of mechanical stretch in the gelatinolytic activity of the fibrous sclera of chicks, in vitro. *Jpn J Ophthalmol.* 2002;46:24–30.
62. Quigley HA, Brown A, Dorman-Pease ME. Alterations in elastin of the optic nerve head in human and experimental glaucoma. *Br J Ophthalmol.* 1991;75:552–557.
63. Friedman DS, Wolfs RC, O'Colmain BJ, et al. Prevalence of open-angle glaucoma among adults in the United States. *Arch Ophthalmol.* 2004;122:532–538.
64. Ollivier FJ, Brooks DE, Kallberg ME, et al. Time-specific intraocular pressure curves in Rhesus macaques (Macaca mulatta) with laser-induced ocular hypertension. *Vet Ophthalmol.* 2004;7:23–27.
65. Rada JA, Shelton S, Norton TT. The sclera and myopia. *Exp Eye Res.* 2006;82:185–200.
66. Fung YC. *Biomechanics: Mechanical Properties of Living Tissues.* 2nd ed. New York: Springer-Verlag; 1993.
67. Weiss JA, Maker BN, Govindjee S. Finite element implementation of incompressible, transversely isotropic hyperelasticity. *Comput Methods Appl Mech Engrg.* 1996;135:107–128.
68. Holzapfel G, Gasser T, Ogden R. A New Constitutive framework for arterial wall mechanics and a comparative study of material models. *J Elasticity.* 2000;61:1–48.
69. Nguyen TD, Jones RE, Boyce BL. A nonlinear anisotropic viscoelastic model for the tensile behavior of the corneal stroma. *J Biomech Eng.* 2008;130:041020.
70. Grytz R, Meschke G. A computational remodeling approach to predict the physiological architecture of the collagen fibril network in corneo-scleral shells. *Biomech Model Mechanobiol.* 2010;9:225–235.
71. Holzapfel GA, Ogden RW. Constitutive modelling of arteries. *Proc R Soc A.* 2010;466:1551–1597.
72. Sigal IA, Ethier CR. Biomechanics of the optic nerve head. *Exp Eye Res.* 2009;88:799–807.
73. Sigal IA. Interactions between geometry and mechanical properties on the optic nerve head. *Invest Ophthalmol Vis Sci.* 2009;50:2785–2795.
74. Roberts MD, Liang Y, Sigal IA, et al. Correlation between local stress and strain and lamina cribrosa connective tissue volume fraction in normal monkey eyes. *Invest Ophthalmol Vis Sci.* 2010;51:295–307.